Using drift scans to improve astrometry with Spitzer

James G. Ingalls, Sean J. Carey, Patrick J. Lowrance, Carl C. Grillmair, and John R. Stauffer

ABSTRACT

The *Spitzer* Space Telescope Infrared Array Camera (IRAC) is the only space-based instrument currently capable of continuous long duration monitoring of brown dwarfs to detect variability and characterize their atmospheres. Any such studies are limited, however, by the accuracy to which we know the positions and distances to these targets (most of which are newly discovered and therefore do not yet have multiple epochs of astrometric data). To that end, we have begun a new initiative to adapt the astrometric drift scanning technique employed by the Hubble Space Telescope to enhance Spitzer measurements of parallaxes and proper motions of brown dwarfs and other targets. A suite of images are taken with a set of sources scanned across the array. This technique reduces random noise by coaddition, and because each target covers multiple pixels we are able to average over residual instrumental distortion and intra-pixel variations. Although these benefits can be realized with appropriate dithering, scanning is much more efficient because we can take data concurrently with the spacecraft motion, covering many pixels without waiting to reposition and settle. In this contribution we demonstrate that the observing mode works and describe our software for analyzing the observations. We outline ongoing efforts towards simultaneously solving for source position and residual distortion. Initial testing shows a factor of more than 2 improvement in the astrometric precision can be obtained with Spitzer. We anticipate being able to measure parallaxes for sources out to about 50 pc, increasing the volume surveyed by a factor of 100 and enabling luminosity measurements of the young population of brown dwarfs in the β Pictoris moving group. This observing mode will be ready for public use around Winter of 2015.

Keywords: methods: data analysis, space vehicles: instruments, techniques: astrometric, observatories: *Spitzer*, spatial scanning

1. INTRODUCTION

The Infrared Array Camera[1] (IRAC) on board the *Spitzer* Space Telescope[2] is one of the few instruments capable of long duration monitoring of brown dwarfs to detect variability and characterize their atmospheres. Any such studies are limited, however, by the accuracy to which we know the positions and distances to these targets (most of which are newly discovered and therefore do not yet have multiple epochs of astrometric data). Because of their faintness, most detectable brown dwarfs are within 100 pc, so their distances are measurable via trigonometric parallaxes, where the position of a star relative to background sources will vary due to the motion of the observatory around the Sun. Nearby stellar kinematical groups[3] contain large numbers of young stars and are considered among the best candidate ensembles to search for brown dwarfs.[4] For example, the β Pictoris moving group, a collection of 17 different star systems aged about 12 Myr, has a distance of $d \sim 35$ pc, implying a parallax of order 30 milliarcseconds (mas). The best precision on brown dwarf parallaxes measured to date with *Spitzer* is 50 mas.[5]

This contribution analyzes the potential of using drift scans to improve the precision of astrometric measurements with *Spitzer* IRAC. Drift scanning in astronomy is the practice of either passively or actively allowing a telescope to drift relative to a celestial object or scene. For *Spitzer* the technique is used actively to move the observatory such that one or more sources are scanned at an approximately constant rate across the detector plane. Also referred to as spatial scanning, this method is currently being used for astrometry with the Hubble Space Telescope (HST) Wide Field Camera 3 (WFC3).[6] There are many crucial differences between WFC3 and IRAC that lead to somewhat different approaches to the observations and data reduction, as described below.

Parallax measurements require precise and accurate measurement of the angular separation between a target star and one or more background stars, over multiple observational epochs spanning months or years. For most

Spitzer Science Center, Infrared Processing and Analysis Center, California Institute of Technology, Mail Code 314-6, Pasadena, CA 91125. Send correspondence to JGI: Email: ingalls@ipac.caltech.edu; Phone: 1 626 395 8659

Space Telescopes and Instrumentation 2014: Optical, Infrared, and Millimeter Wave, edited by Jacobus M. Oschmann, Jr., Mark Clampin, Giovanni G. Fazio, Howard A. MacEwen, Proc. of SPIE Vol. 9143, 91431M · © 2014 SPIE
CCC code: 0277-786X/14/$18 · doi: 10.1117/12.2056755

imaging systems, optical distortion over the field of view is the primary source of positional error in a given measurement of a point source. In addition, unlike WFC3 which is fully sampled, the *Spitzer* IRAC optical point spread functions (PSFs) at both 3.6 μm and 4.5 μm (FWHM $\sim 1\farcs4$ for each) are undersampled by about 70% (the pixel size is $\sim 1\farcs2$). This leads to positional errors that vary with intra-pixel position, or pixel *phase* (defined as zero at the center of a pixel and ± 0.5 at the edge).[7] We will refer to these errors here as "intra-pixel distortion," (IPD) since the outcome is analogous to array-wide distortion, in that measured centroids are shifted with respect to where the stellar center would be in a perfect system. We emphasize, however, that the cause of IPD is not optical distortion of light, but rather our inability to locate accurately the center of light due to detector undersampling.

To improve astrometric precision, it is thus beneficial to move sources around the array to average over differences in array-wide and intra-pixel distortion, while building up signal-to-noise and mitigating bad pixels. Spatial "dithering" on a pre-defined pattern is a standard operating mode for IRAC.

Spatial *scanning*, heretofore unused for astrometry with *Spitzer*, has two main benefits over dithering: (1) it is more efficient—the repositioning of the telescope occurs concurrently with data acquisition, so the same number of photons can be collected in less time (in practice, about 1/2 as much time); (2) the motion is continuous, so a star will smoothly sample entire pixels along the scan direction, guaranteeing that the entire range of pixel phase (and hence IPD) is covered. We find that even when a scan is commanded parallel to one of the array axes, its path actually makes a small angle with respect to the axis such that (for a full 256-pixel scan) a star traverses more than 1 complete pixel in the perpendicular direction as well. This is unlike dithering, where the placement of a point source on the array suffers from an initial ~ 1 px pointing error, in addition to a 0.1 px error in each subsequent dither offset, making it difficult to intentionally sample a sufficiently diverse range of pixel phase. The one potential drawback to scanning is that, along the scan direction the image may become too spread out to allow the localization of stars in that direction. This problem can be reduced by taking multiple short images in succession, such that individual images do not smear the PSF by more than a few pixels (see below).

In this paper we begin by outlining test measurements that were taken as part of the IRAC calibration program, as well as our software for reducing the data (§2). We describe in §3 how we derived the intra-pixel distortion correction using simulated images built from the IRAC point response function (PRF). We show the results of our tests in §4, where we demonstrate successful correction for array and intra-pixel distortion and measure angular separations perpendicular to the scan direction. In §5 we discuss implications of these results for estimating parallaxes and proper motions. We summarize in §6 the current state of work and indicate future work that is necessary before drift scans can be used for astrometry with *Spitzer*.

2. METHODOLOGY

2.1 Designing Drift Scans

Drift scan measurements with *Spitzer* use a spacecraft command that scans an instrument field of view (FOV) for a specified duration at specified rates along the horizontal (u) and/or vertical (v) pixel axes. While the scan is taking place, one or more IRAC arrays are exposed, producing a suite of images at a specified integration time. Images are taken back to back throughout the scan. The scanning command is currently only accessible via Instrument Engineering Requests (IERs) authored by an IRAC instrument scientist, and not through the publicly available *Spitzer* Planning Observations Tool (Spot). The IERs can be converted into observing templates for Spot if there is sufficient demand from the user community.

In addition to the drift direction(s) and duration(s), two important parameters are required for any drift scan observation: scan rate R [from 0 to 6000 milliarcseconds per second (mas s^{-1}) is allowed for *Spitzer*] and per-frame integration time $t_{\rm frame}$ (in seconds). Note that R, not $t_{\rm frame}$, affects how much light falls on each pixel, which governs the sensitivity and saturation potential of a given observation. We relate the scan rate along an axis to the integration time for regular pointed observations, $t_{\rm pointed}$, by requiring that sources travel about 3 pixels ($3\farcs6$) in $t_{\rm pointed}$. This is somewhat arbitrary but it is based on the fact that the bulk of the photon flux from a point source falls on a 3×3 pixel box. It should ensure that a source neither saturates or becomes too dilute in any given pixel. Thus

$$\frac{R}{\rm mas\ s^{-1}} \sim \frac{3.6 \times 10^3}{t_{\rm pointed}}. \quad (1)$$

The per-frame integration time constrains the amount of smearing that occurs in each image frame due to the scanning motion. Given that the PSF is undersampled by IRAC, a certain amount of smearing is beneficial because it reduces intrapixel effects that lead to photometric gain variations and centroid measurement bias. We assert then that a reasonable value for $t_{\rm frame}$ is that for which the smeared PSF is fully sampled along the scan direction. In other words the distance traveled over the course of the integration, $R\,t_{\rm frame}/1000$, should be approximately twice the pixel size, $2\farcs4$, or:

$$t_{\rm frame} \sim \frac{2400}{R}\,{\rm s}. \tag{2}$$

The integration can be slightly larger than this without ill effect; it does not hurt to be a bit oversampled. Keep in mind, however, that if $t_{\rm frame}$ increases too much then the smearing will result in an unmeasurable centroid.

2.2 Test Measurements of NGC 2516

In May and September 2013, we ran tests of drift scanning on a portion of the NGC 2516 open cluster. The cluster's distance is 360 pc,[8] so angular separations between cluster members and background stars should not change more than about 3 mas from epoch to epoch, an order of magnitude smaller than the brown dwarf parallaxes we wish to measure.

We scanned the center of the cluster across the Channel 2 array (bandpass centered on 4.5 μm). We estimated that a pointed integration time of $t_{\rm pointed} = 12$ s would ensure the detectability of many of the fainter sources while still not saturating the brighter ones. Thus a scan rate of 300 mas s^{-1} satisfies Equation 1. Substituting into Equation 2, a fully sampled smeared PSF along the scan direction requires that $t_{\rm int}$ be no less than 8 s. The closest (larger) IRAC frame time is $t_{\rm int} = 12$ s.

In our experiment, we scanned in both horizontal, vertical, and diagonal directions with respect to the IRAC arrays. For the horizontal and vertical scans, we scanned such that a star in the center of either array would first move to one edge, reverse direction and move to the other edge, then reverse and return to the center. The May and September epochs repeated this experiment 4.5 months apart, with the only difference being that the focal plane was significantly rotated (about 135°) between epochs due to *Spitzer*'s sunshade roll angle constraint.

2.3 Reducing Drift Scan Data

All results described herein use images of the NGC 2516 cluster taken while scanning at $R = \pm 300$ mas s^{-1} along either the horizontal or vertical axis of warm IRAC Channel 2 (4.5 μm). The images were processed by the IRAC data reduction pipeline and are available from the *Spitzer* Heritage Archive (Program 1342) in the form of *Spitzer* basic calibrated data (BCD) FITS files.

We processed further all images using a software package, `drift_analyze`, written in the IDL language. The program displays the first 12s exposure in the set and allows the user to scale the display intensities, optionally load a list of previously selected stars, and overlay symbols at the location of each star. One may interactively select or deselect stars from the overlay using the computer mouse. Finally, when the list has been decided, a button is clicked and the program loads each subsequent 12s image frame taken during the scan and automatically finds the new position of each star. Each new image is averaged with the previous ones, appearing as growing star trails on the display. Screenshots of `drift_analyze` in action are shown in Figure 1.

The software computes the centroid positions (u_{ij}, v_{ij}) of star i in frame j by measuring the intensity-weighted mean pixel in a box:

$$u_{ij} = \frac{\sum_{l,m}(I_{lm}\,l)}{\sum_{l,m} I_{lm}} \tag{3}$$

$$v_{ij} = \frac{\sum_{l,m}(I_{lm}\,m)}{\sum_{l,m} I_{lm}}. \tag{4}$$

Here I_{lm} is the (background subtracted) surface brightness in the pixel located at (column,row) = (l, m), where the coordinates start at (0,0) at the bottom left corner of the array. In these coordinates, a whole number value

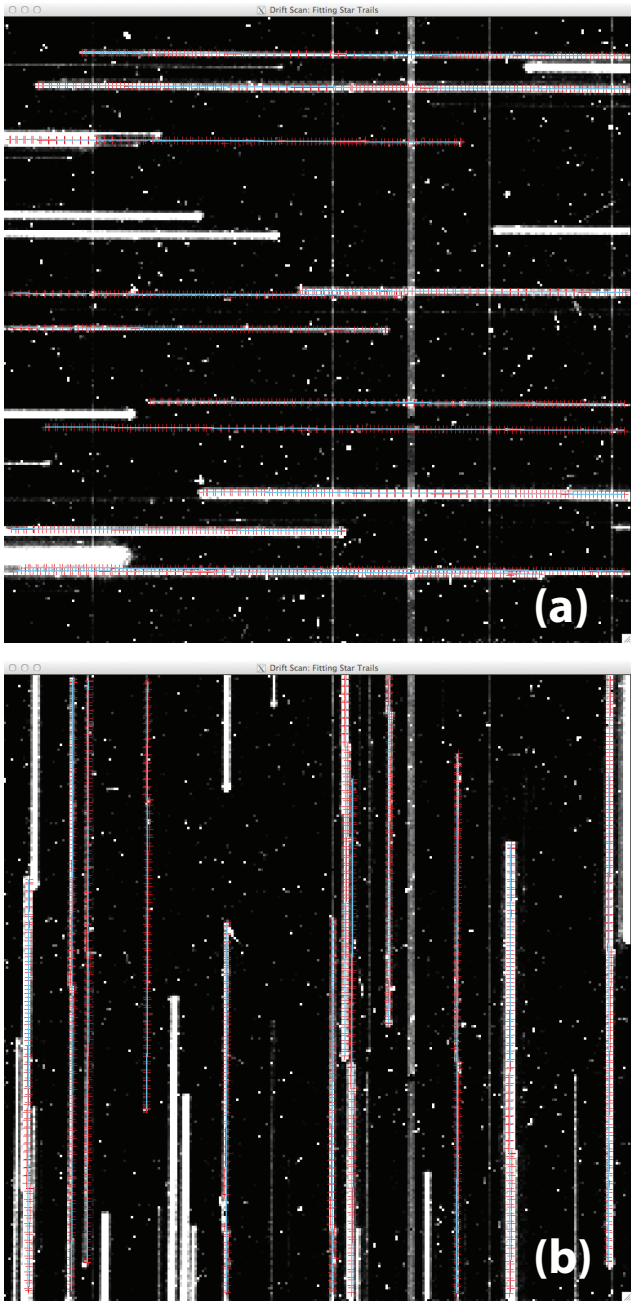

Figure 1. Screen shots from two sessions of `drift_analyze`, from the Epoch 1 (May 2013) data for NGC 2516. (*a*) Drift scans in the u direction. (*b*) Drift scans in the v direction. These images are the average over all individual frames in the scan. Superimposed are "+" symbols showing each measured centroid position from each frame. Blue lines represent linear fits to each star trail, an optional output of the program. Grayish vertical "stripes" in both images are a column pulldown artifact due to permanently hot pixels.

for u or v would mean that the target was at the center of a pixel. The sums were truncated to a 7×7-pixel box around the expected position of the source. For the first frame in the scan ($j = 0$), expected positions are the user-selected locations (either chosen by mouse click or loaded from a file); for subsequent frames j, the expected

positions are simply the positions from the previous frames, $(u_{i,j-1}, v_{i,j-1})$. The complete set of measurement times, the positions of each star and their uncertainties and covariances, $\{t_{ij}, u_{ij}, v_{ij}, \sigma_{u_{ij}}, \sigma_{v_{ij}}, \sigma_{uv_{ij}}\}$, are stored in a file.

2.4 From Pixel to Projection Plane Coordinates

Our goal is to measure angular separations on the sky between stars in the images. We use the conversion between pixel and "intermediate world coordinates," or projection plane coordinates, specified in the FITS format standard,[9] augmented for *Spitzer* array-wide distortion via the Simple Imaging Polynomial (SIP) keywords.[10] In this standard, the coordinates (x, y) are angular distances on a plane tangent to the position on the celestial sphere given by the FITS header keywords (`CRVAL1`,`CRVAL2`). In an astronomical image, this position is located at pixel (`CRPIX1`,`CRPIX2`). A 2×2 "CD matrix" is one component of the pixel to sky coordinate conversion, containing the linear terms in the relationship between (u, v) and (x, y). This encodes the pixel scale (degrees per pixel), coordinate rotation, and pixel skew (non-rectangularity between the pixel axes). A "Distortion matrix" contains nonlinear terms. We now add to this transformation a function to correct for intrapixel distortion (IPD), which is not part of the FITS standard because it does not apply to the pixel grid but rather corrects a bias in centroid measurements at the sub-pixel level.

The relationship between pixel position (u, v) and projection plane coordinates on the sky (x, y) is given by:

$$\begin{pmatrix} x \\ y \end{pmatrix}_{ij} = \begin{pmatrix} \texttt{CD1\_1} & \texttt{CD1\_2} \\ \texttt{CD2\_1} & \texttt{CD2\_2} \end{pmatrix}_{j} \begin{pmatrix} u'_{\rm rel} \\ v'_{\rm rel} \end{pmatrix}_{ij} . \tag{5}$$

Here u_{ij} and v_{ij} are the measured centroids for star i on frame j. We drop ij subscripts in what follows.

The primes in Equation 5 imply correction for (1) intrapixel distortion:

$$\begin{pmatrix} u_{\rm IPD} \\ v_{\rm IPD} \end{pmatrix} \equiv \begin{pmatrix} u \\ v \end{pmatrix} - F_{\rm IPD} \left[\begin{pmatrix} u \\ v \end{pmatrix} \right] ; \tag{6}$$

and (2) array-wide distortion (using the SIP convention):

$$\begin{pmatrix} u'_{\rm rel} \\ v'_{\rm rel} \end{pmatrix} \equiv \begin{pmatrix} u_{\rm rel} \\ v_{\rm rel} \end{pmatrix} + \sum_{p,q} \begin{pmatrix} A_{pq} \\ B_{pq} \end{pmatrix} u_{\rm rel}^{p} v_{\rm rel}^{q} \quad . \tag{7}$$

Here the subscript "rel" indicates that the pixel coordinates are relative to (`CRPIX1`,`CRPIX2`):

$$\begin{pmatrix} u_{\rm rel} \\ v_{\rm rel} \end{pmatrix} \equiv \begin{pmatrix} u_{\rm IPD} \\ v_{\rm IPD} \end{pmatrix} - \begin{pmatrix} \texttt{CRPIX1} \\ \texttt{CRPIX2} \end{pmatrix} . \tag{8}$$

The summation indices in Equation 7 are constrained by the FITS header keywords `A_ORDER` and `B_ORDER`, corresponding to A_{pq} and B_{pq}, respectively:

$$2 \ \leq \ (p+q) \ \leq \ \begin{pmatrix} \texttt{A\_ORDER} \\ \texttt{B\_ORDER} \end{pmatrix} ; \ p \geq 0; \ q \geq 0. \tag{9}$$

The intrapixel distortion function, $F_{\rm IPD}$, is the subject of the following section.

3. CORRECTING INTRA-PIXEL DISTORTION

As described in the introduction, we correct for a bias function, the intrapixel distortion (IPD), which reflects the inability to determine accurately the center of light when the PSF is under-sampled. We derive the function $F_{\rm IPD}$ empirically using the published IRAC point response functions (PRFs), tabulated images of point sources at specified sub-pixel offsets (pixel phase). Since the PSF varies with position across a given IRAC array, $F_{\rm IPD}$ depends on both the pixel phase and the absolute position. To derive $F_{\rm IPD}$ for drift scan images we use `iracsim`, a data simulator that mimics real IRAC detector sampling as a function of time and allows for moving sources.

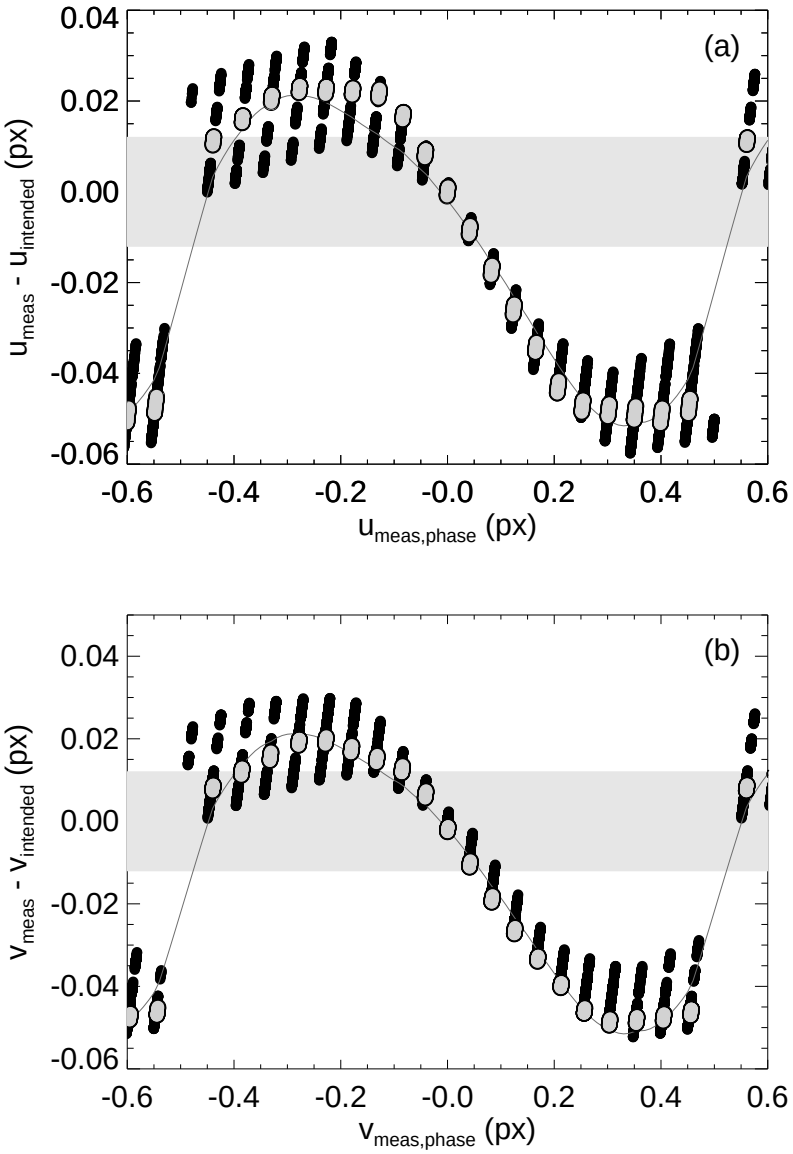

Figure 2. Intrapixel "Distortion" (IPD) along a non-scanned axis in simulated point source images on the IRAC 4.5 μm array. (a) Offsets along the horizontal pixel axis u. (b) Offsets along the vertical axis v. These plots display the discrepancy between the measured intensity-weighted centroid and the intended position, as a function of the measured pixel phase. Black filled circles show the totality of data taken on a grid of equally-spaced positions across the entire array. Light gray circles show only the measurements centered on $(u, v) = (129,129)$. We simulated a range of pixel phases in u and v for each array location. The very narrow vertical spread in the light gray circles demonstrates that there is little dependence of IPD in a given direction on pixel phase along the orthogonal direction. We overlay smooth curves showing the u and v functions, $F_{\rm IPD}$, used to correct actual drift scan data for array location (129,129). Similar curves were derived for each location on the simulation grid. A gray band bounds the expected angular separation that will need to be resolved to measure parallaxes towards the β Pictoris moving group.

Although the simulator includes a detailed *Spitzer* pointing model with jitter and other known effects,[12] we turn off all pointing behavior to isolate the IPD.

For this paper, we concern ourselves only with measuring separations *perpendicular* to the scan direction

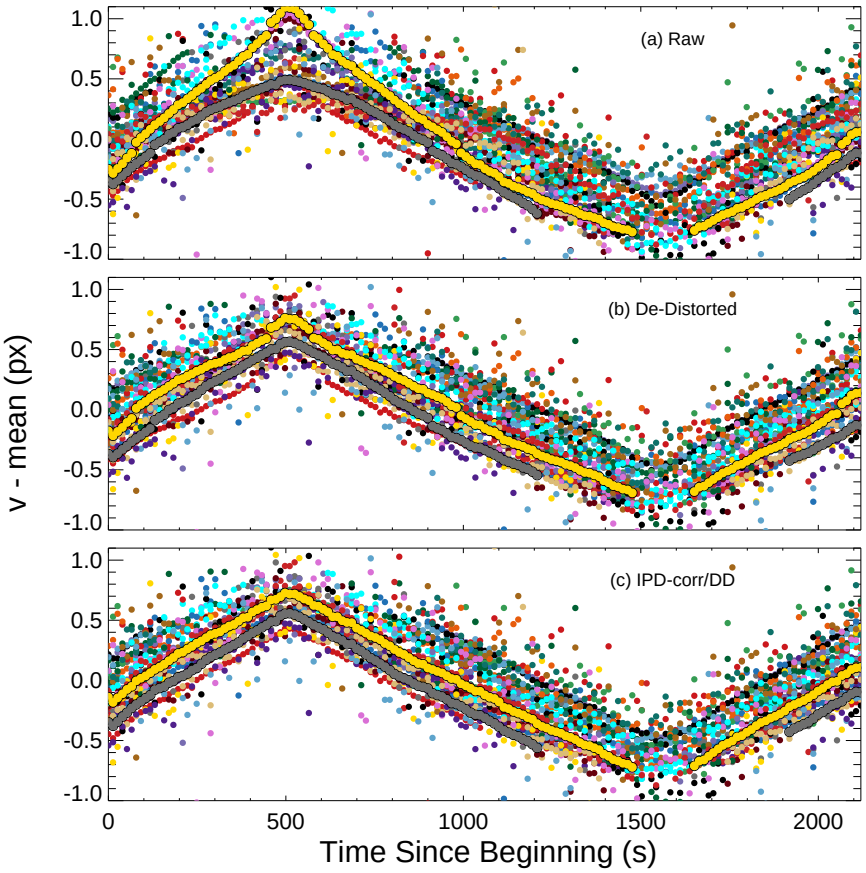

Figure 3. Centroids along the v (vertical) pixel axis as a function of time for drift scans along the u axis. The three panels show data processed in three ways: (a) raw centroids (Equation 4) measured directly on the images; (b) centroids corrected only for array-wide distortion (Equation 7), using the 3rd order SIP coefficients provided with all *Spitzer* IRAC data; and (c) centroids corrected for first intrapixel and then array-wide distortion (Equation 6). Colors represent different stars. We highlight the measurements for stars labeled 0 (yellow; also known as CD-60 1954) and 7 (gray; V*V417 Car). The mean centroid for each star has been subtracted from each value of v.

(*i.e.,* v separations for u scans and vice-versa). We have confirmed in simulation that if a target is moving in one direction it does not affect centroid measurements along the orthogonal non-scanned direction. We used `iracsim` to produce simulated images with the source located at different positions on the array, and on a grid of pixel phases. We then measured the centroids for each of these images (Equations 3 and 4) and compared the values to the intended positions.

The results are shown in Figure 2. The IPD can be as much as 5% of a pixel, or 60 mas, which is significant compared to the angular separation of 29 mas that must be resolved to measure parallaxes towards the β Pictoris moving group (gray band in Figure 2). To correct centroids in real data, we derive $F_{\rm IPD}$ using Krige fitting[11] to the simulated data (smooth curves in Figure 2). We then tabulated $F_{\rm IPD}$ for a grid of array locations and pixel phases (along the direction whose IPD is being calculated) so we could use trilinear interpolation to estimate $F_{\rm IPD}$ for a given data point.

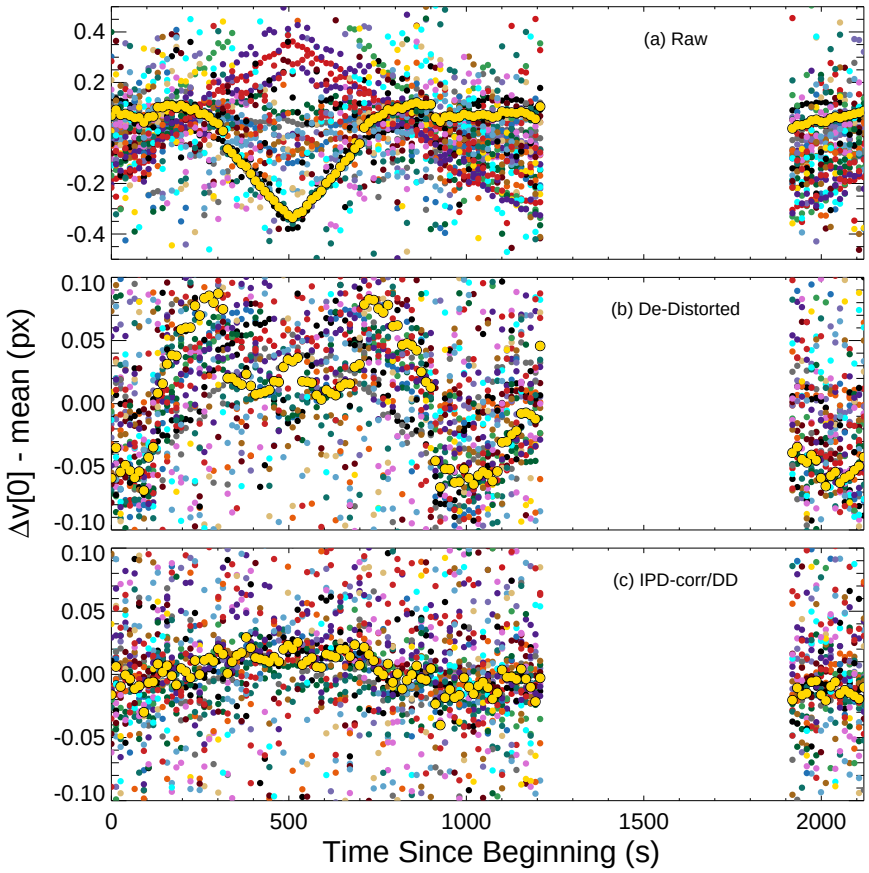

Figure 4. Centroids relative to Star 7 (V*V417 Car) along the v (vertical) pixel axis as a function of time for drift scans along the u (horizontal) axis. The three panels show data processed as per Figure 3. Note the larger ordinate range in panel(a). Colors represent different stars. We highlight the measurements for Star 0 (CD-60 1954) in yellow. The mean difference for each star has been subtracted from each value of v.

4. DRIFT SCAN RESULTS

4.1 Positions in the Cross-Scan Direction

We plot the v centroids as a function of time for the u drift scans of Epoch 1 (May 2013) in Figure 3. To demonstrate the affect of the distortion corrections, we show three versions of processing: raw, corrected for array-wide distortion only, and corrected for first intrapixel and then array-wide distortion. In an ideal observatory without telescope jitter, the curves for any two stars should be parallel to each other, and this comes closest to happening for the data with both distortion corrections.

4.2 Separation Measurements

Figure 4 graphs v separations between per-frame centroids of Star 7 (V*V417 Car) and those of each of the remaining 35 stars we have chosen. The three panels follow the same processing as in Figure 3. Histograms of centroid differences between Stars 0 (CD-60 1954) and 7 (V*V417 Car) are displayed in Figure 5. The data with both intrapixel and array-wide distortion correction have a much narrower distribution and are more symmetrically distributed than the data only corrected for array-wide distortion. The IPD-corrected distribution has only one peak; the other distributions do not.

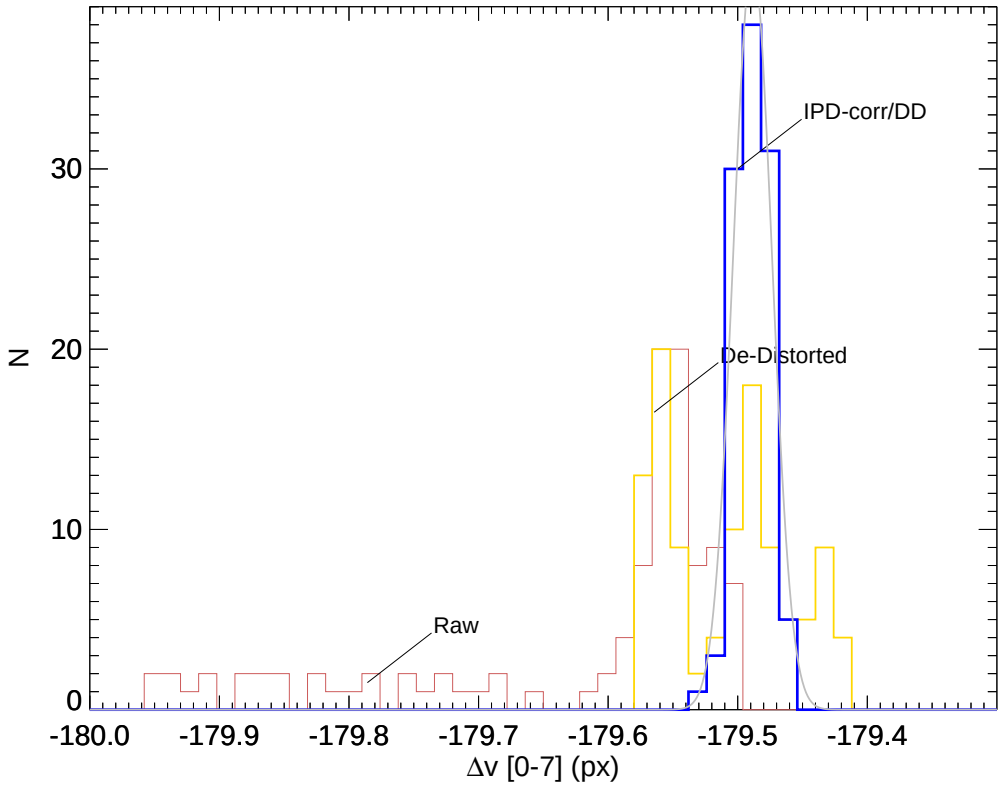

Figure 5. Histograms of centroid differences between Stars 0 and 7, measured along the v pixel axis for drift scans along the u axis. Data have been processed as per Figure 3: (1) raw centroids (red); (2) centroids corrected for array-wide distortion only (yellow); and (3) centroids corrected for first intrapixel and then array-wide distortion (blue). The smooth gray curve represents a gaussian fit to (3), with center at -179.489 pixels and standard deviation 0.015 pixels.

5. ASTROMETRIC MEASUREMENTS

Only the data with IPD correction are capable of resolving changes in angular separation of ~ 29 mas. Naively, histograms like those shown in Figure 5 can be converted into astrometric measurements by scaling from pixel to sky coordinates. For example, fitting a gaussian to the IPD-corrected histogram gives a centroid of $\Delta v = -179.489$ px and standard deviation of $\sigma_v = 0.015$ px. Doing the same with a histogram of the u centroid differences from v scans for the same two stars (Epoch 1) yields $\Delta u = 49.223$ px and $\sigma_u = 0.017$ px. Multiplying by the pixel scale for each dimension and adding in quadrature gives an angular separation of $\Delta_1 = 226\farcs297 \pm 0\farcs018$. However, the same measurement on same the two stars in October 2013 (Epoch 2) yields an angular separation of $\Delta_2 = 224\farcs474 \pm 0\farcs017$. The known parallaxes and proper motions on the two stars, which are in the Tycho database, cannot account for $1\farcs8$ of motion over 4.5 months!

One possibility that needs to be investigated is that the optical distortion solution currently in use is inadequate for scanned data. The fact that we are unable to reproduce an astrometric measurement when the field has rotated by $-135°$ might be due to an error in the large scale behavior of the distortion polynomials. The distortion correction averages $1\farcs6$ across the array, so a small change in one of the lower order terms might be responsible for $1\farcs8$ discrepancy between the two Epochs.

We surmise further that intrapixel and array-wide distortion are not the only impediments to converting from pixel to sky projection plane coordinates. In addition to the pixel scale, the CD matrix (Equation 5) also contains

field rotation and pixel skew, which we have not yet accounted for. Skew is constant over time and should not affect measurements primarily along pixel axes. However, we have implicitly assumed that the rotation from frame to frame within a given epoch was also constant. Analysis of drift scans with Hubble Space Telescope WFC3 found that instantaneous changes in the roll angle produced non-parallel stellar trails, which needed to be taken into account to convert properly to sky coordinates.[6]

6. SUMMARY

Drift scans are a new technique for astrometry with *Spitzer*, to estimate parallaxes and proper motions of nearby sources. In this paper, we discuss how to plan drift scan measurements, and give the example of our test measurements of open cluster NGC 2516. We introduce the concept of intrapixel "distortion" (IPD), which is a significant systematic in the measurement of angular separations at the < 100 mas level. We demonstrate that correcting for IPD as well as the array-wide optical distortion in the NGC 2516 data reduces the systematics substantially and yields a distribution in stellar separation values in the cross-scan direction with standard deviation < 20 mas, much better than with the optical distortion correction alone. We cannot, however, reproduce angular separations from one observing epoch to another. We are currently investigating (1) possible refinement of the optical distortion solution; and (2) instantaneous roll angle as an additional variable to compute and account for.

ACKNOWLEDGMENTS

This work is based on observations made with the *Spitzer* Space Telescope, which is operated by the Jet Propulsion Laboratory, California Institute of Technology under a contract with NASA.

REFERENCES

[1] Fazio, G. G., Hora, J. L., Allen, L. E., Ashby, M. L. N., Barmby, P., Deutsch, L. K., Huang, J.-S., Kleiner, S., Marengo, M., Megeath, S. T., Melnick, G. J., Pahre, M. A., Patten, B. M., Polizotti, J., Smith, H. A., Taylor, R. S., Wang, Z., Willner, S. P., Hoffmann, W. F., Pipher, J. L., Forrest, W. J., McMurty, C. W., McCreight, C. R., McKelvey, M. E., McMurray, R. E., Koch, D. G., Moseley, S. H., Arendt, R. G., Mentzell, J. E., Marx, C. T., Losch, P., Mayman, P., Eichhorn, W., Krebs, D., Jhabvala, M., Gezari, D. Y., Fixsen, D. J., Flores, J., Shakoorzadeh, K., Jungo, R., Hakun, C., Workman, L., Karpati, G., Kichak, R., Whitley, R., Mann, S., Tollestrup, E. V., Eisenhardt, P., Stern, D., Gorjian, V., Bhattacharya, B., Carey, S., Nelson, B. O., Glaccum, W. J., Lacy, M., Lowrance, P. J., Laine, S., Reach, W. T., Stauffer, J. A., Surace, J. A., Wilson, G., Wright, E. L., Hoffman, A., Domingo, G., and Cohen, M., "The Infrared Array Camera (IRAC) for the Spitzer Space Telescope," *The Astrophysical Journal Supplement Series* **154**, 10–17 (Sept. 2004).

[2] Werner, M. W., Roellig, T. L., Low, F. J., Rieke, G. H., Rieke, M., Hoffmann, W. F., Young, E., Houck, J. R., Brandl, B., Fazio, G. G., Hora, J. L., Gehrz, R. D., Helou, G., Soifer, B. T., Stauffer, J., Keene, J., Eisenhardt, P., Gallagher, D., Gautier, T. N., Irace, W., Lawrence, C. R., Simmons, L., Van Cleve, J. E., Jura, M., Wright, E. L., and Cruikshank, D. P., "The Spitzer Space Telescope Mission," *The Astrophysical Journal Supplement Series* **154**, 1–9 (Sept. 2004).

[3] Zuckerman, B. and Song, I., "Young Stars Near the Sun," *Annual Review of Astronomy &Astrophysics* **42**, 685–721 (Sept. 2004).

[4] Luhman, K. L., "The Formation and Early Evolution of Low-Mass Stars and Brown Dwarfs," *Annual Review of Astronomy and Astrophysics* **50**, 65–106 (Sept. 2012).

[5] Beichman, C., Gelino, C. R., Kirkpatrick, J. D., Cushing, M. C., Dodson-Robinson, S., Marley, M. S., Morley, C. V., and Wright, E. L., "WISE Y Dwarfs as Probes of the Brown Dwarf-Exoplanet Connection," *The Astrophysical Journal* **783**, 68 (Mar. 2014).

[6] Riess, A. G., Casertano, S., Anderson, J., MacKenty, J., and Filippenko, A. V., "Parallax beyond a Kiloparsec from Spatially Scanning the Wide Field Camera 3 on the Hubble Space Telescope," *The Astrophysical Journal* **785**, 161 (Apr. 2014).

[7] Mighell, K. J., Glaccum, W., and Hoffmann, W., "Improving the photometric precision of IRAC Channel 1," *Space Telescopes and Instrumentation 2008: Optical* **7010**, 86 (Aug. 2008).

[8] Sung, H., Bessell, M. S., Lee, B.-W., and Lee, S.-G., "The Open Cluster NGC 2516. I. Optical Photometry," *The Astronomical Journal* **123**, 290–303 (Jan. 2002).

[9] Calabretta, M. R. and Greisen, E. W., "Representations of celestial coordinates in FITS," *Astronomy and Astrophysics* **395**, 1077–1122 (Dec. 2002).

[10] Shupe, D. L., Moshir, M., Li, J., Makovoz, D., Narron, R., and Hook, R. N., "The SIP Convention for Representing Distortion in FITS Image Headers," *Astronomical Data Analysis Software and Systems XIV ASP Conference Series* **347**, 491 (Dec. 2005).

[11] Rybicki, G. B. and Press, W. H., "Interpolation, realization, and reconstruction of noisy, irregularly sampled data," *Astrophysical Journal* **398**, 169–176 (Oct. 1992).

[12] Grillmair, C. J., Carey, S. J., Stauffer, J. R., Fisher, M. E., Olds, R., Ingalls, J. G., Krick, J. E., Glaccum, W. J., Laine, S., Lowrance, P. J., and Surace, J. A., "Pointing effects and their consequences for Spitzer IRAC exoplanet observations," in [*SPIE Observatory Operations: Strategies, Processes, and Systems IV*], 84481I–84481I–9, SPIE (Sept. 2012).